Preprints of the 19th World Congress
The International Federation of Automatic Control
Cape Town, South Africa. August 24-29, 2014

Improving the positioning bandwidth of the Integral Resonant Control Scheme through strategic zero placement.

Douglas Russell * **Andrew J. Fleming** ** **Sumeet S. Aphale** *

* *Centre for Applied Dynamics Research, School of Engineering, University of Aberdeen, UK*
** *Centre for Complex Dynamic Systems and Control, School of Electrical Engineering and Computer Science, University of Newcastle, Australia*

Abstract: Integral Resonant Control (IRC) is a simple and robust control scheme for vibration damping. Combined with an integral tracking controller, the IRC has been shown to improve the performance of a wide range of nanopositioners. However, the overall improvement in positioning performance is limited by the pole induced by the IRC. Through selective zero placement, the induced pole can be placed near origin. A structured PI tracking controller, where the PI gains are selected to place a zero at a specific location, is used to cancel the pole. This effectively reduces the order of the system by one. For this system, controller gains are derived analytically in order to maximize tracking bandwidth. Simulation results for one axis of a nanopositioner are provided for both standard and modified IRC schemes. Compared to the standard IRC scheme, the modified IRC scheme is found to provide a 55% increase in the $\pm 1\ dB$ bandwidth and a reduction of both maximum and rms tracking errors.

1. INTRODUCTION

Resonance can drastically reduce the performance characteristics and lifetime of mechatronic systems [Preumont (1997)]. A multitude of vibration damping techniques have been used to suppress the oscillatory nature of such systems, which fall into one of two categories: open- and closed-loop. Open-loop controllers, though simple in their design, often exhibit less than desirable performance and reduced robustness properties. Closed-loop controllers, whilst more complex, provide a vast array of options to fine-tune the performance characteristics of a given system and in general outperform open-loop systems [Inman (1989)].

A number of closed-loop controllers have found widespread use in vibration damping problems, the most common of which being: Positive Position Feedback (PPF) [Fanson and Caughey (1990)], polynomial-based control (also known as Positive Velocity and Position Feedback - PVPF) [Bhikkaji et al. (2007)], Resonant control [Pota et al. (2002)], robust control [Salapaka et al. (2002)], and Integral Resonance Control (IRC) [Aphale et al. (2007)]. These controllers have been implemented in many different applications, including robotic manipulators [Gomes et al. (2006)], disk-drives [Numasato and Tomizuka (2003)], aircraft wings [Friedmann and Millott (1995)], nanopositioning stages [Devasia et al. (2007)], Scanning Probe Microscopes [Fleming et al. (2010)], and high-density memory storage devices [Sebastian et al. (2008)].

Nonlinear behaviour caused by piezoelectric components must also be taken into account. Positioning errors of up to 15% between opposing directional movements, due to hysteresis, creep and thermal drift, have been reported in the literature. To minimize these errors some form of reference tracking is generally incorporated [Devasia et al. (2007)]. The use of a tracking controller with integral action has been shown experimentally to reduce positioning errors due to nonlinear effects, see Aphale et al. (2008); Bhikkaji et al. (2007); Fleming (2010).

As IRC has seen successful implementation in a range of applications, it is desirable to increase performance further without sacrificing its existing advantages, i.e. simple low-order design and robust performance. In this work, a modified IRC scheme is used which makes use of a proportional tracking controller, rather than an integral tracking controller, to reduce the order of the system. This has the benefit of simplifying the mathematical properties of the system which, in turn, increases the ease of manipulating system properties through the choice of controller parameters. It also simplifies the relationship between the damping and tracking controllers. Historically, the design of damping and tracking controllers has been done sequentially. However, it has been shown that they are interrelated, see Namavar et al. (2013). Utilising this knowledge, we can exploit the simple mathematics of the system to derive the relationship and maximize performance.

This paper is structured as follows: in Section II, an overview is given of the current understanding of the IRC scheme and its design procedure. Section III gives a brief overview of the modified IRC scheme. This section also details the reasons for the selection of the feed-through parameter. Section IV describes the analytical derivation of controller parameters which provide a flat band response. Simulated responses of a nanopositioner for a triangle wave reference signal are provided in Section V for both the standard and modified systems and performance

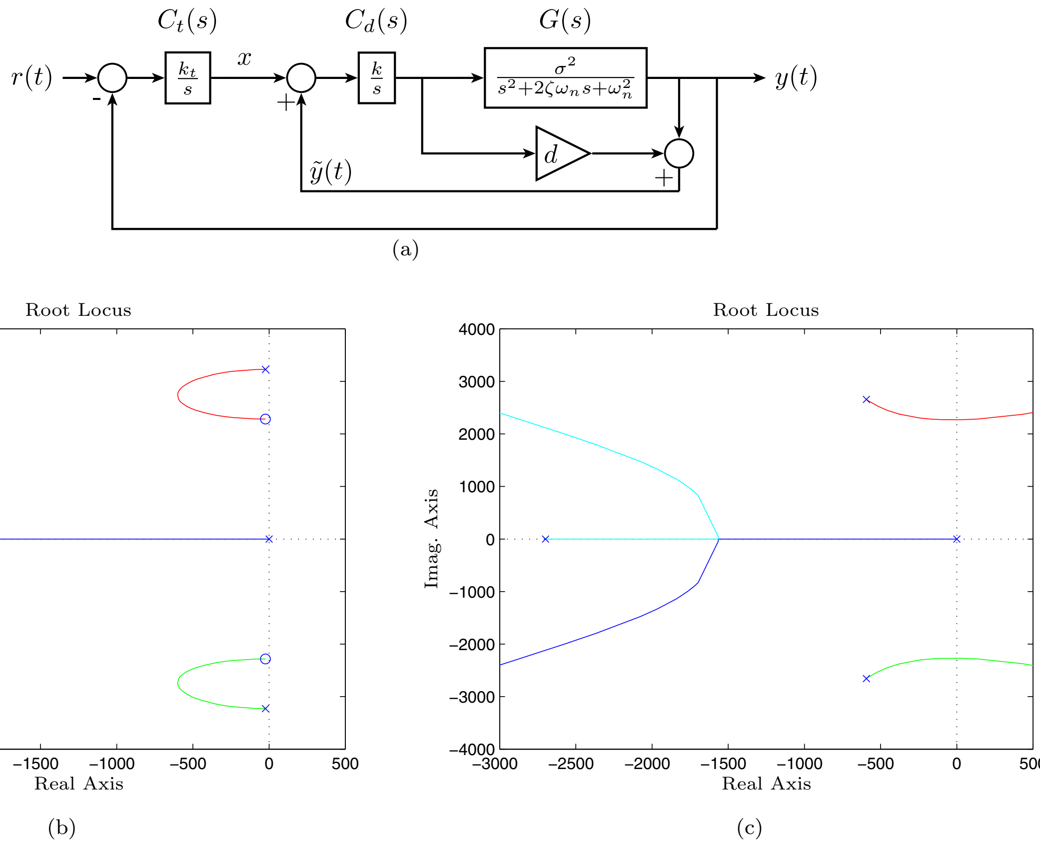

Fig. 1. (a) Block diagram of the damped and tracked IRC scheme where $G(s)$ is the plant, modelled as a lightly damped second-order transfer function, d is the feed-through, $C_d(s)$ is the damping controller, and $C_t(s)$ is the tracking controller. (b) Root locus for the damped standard IRC loop measured from x to $\tilde{y}$. Damping gain, k, can be found form the root locus as the point which provides maximum damping or can be calculated mathematically using Namavar et al. (2013). (c) Root locus for the damped and tracked standard IRC measured from r to y. The tracking loop requires feedback from the direct output of the plant. This causes the change in system output from $\tilde{y}$ to y. This system becomes unstable for large tracking gains, k_t. A maximum for k_t has been derived previously in Namavar et al. (2013).

compared. A detailed analysis of the robust performance delivered by the proposed control scheme, in the presence of resonance frequency changes, is presented in Section VI. Section VII concludes the paper.

2. INTEGRAL RESONANT CONTROL

IRC has found wide use in applications such as cantilever beams [Aphale et al. (2007)], flexible robotic manipulators [Pereira et al. (2011)], nanopositioning platforms [Wadikhaye et al. (2012)], commercial atomic force microscopes [Fleming et al. (2010)], flexible civil structures [Basu and Nielsen (2011)], and walking-induced floor vibrations [Diaz et al. (2012)], due to the simplicity of its design and robust performance. Recent mathematical analysis [Namavar et al. (2013)], has removed the trial-and-error approach to choosing the controller parameters and instead provides criteria required to attain high levels of performance, these include the feed-through and damping gain associated with maximum damping, and maximum tracking gain for stable performance. As Fig. 1(a) shows, the IRC scheme consists of three components: a feed-through term, d, a damping controller, and a tracking controller, both of which are integral controllers.

3. MODIFIED INTEGRAL RESONANT CONTROL SCHEME

In the standard IRC scheme we observe the two damped complex poles of the plant in addition to two real poles induced by the damping and tracking controllers. As the tracking gain, k_t, increases the real poles diverge from the real axis and become complex, see Fig. 1(c). For tracking gain in the range of interest, i.e. that which provides stability, the damping controller-induced pole moves towards the origin rather than away, which is undesirable. The aim of the modified IRC is to remove the non-zero real pole in the damped and tracked root locus. This control scheme should behave like a simple integral controlled system whilst also providing the damping and tracking benefits of standard IRC. In the modified IRC scheme, the damping controller is the same as in standard IRC, and but a proportional tracking controller is used as opposed to the standard integrator, i.e.

$$C_t(s) = k_p. \tag{1}$$

The damped and tracked modified IRC scheme has closed-loop transfer function as given by Eqn. (2).

$$H_{num}(s) = k_p k \sigma^2$$

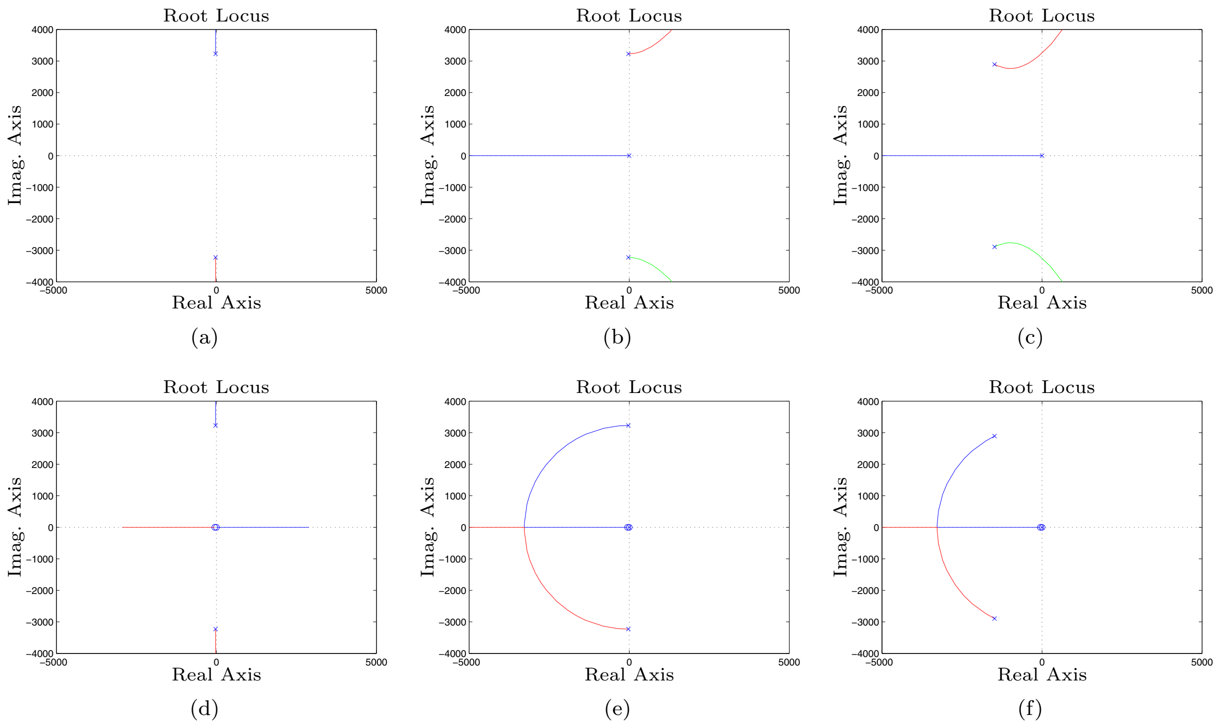

Fig. 2. Root loci for the design procedure of a modified IRC scheme for Case 1. The top row ((a), (b), and (c)) has output y, whereas the bottom row ((d), (e), and (f)) has output $\tilde{y}$, see Fig. 1(a). (a), (d) shows the plant with feed-through, d, added, (b), (e) shows the addition of the damping controller, and (c), (f) the addition of the tracking controller. (e) and (c) are typically used in IRC design, the former to select damping gain, and the latter to choose tracking gain. (e) shows a pole/zero pair located at the origin which prevents displacement of the damping controller induced pole. The two complex poles can be positioned using the damping gain, k, under the condition given in Eqn. (7). (c) shows that there is an upper bound on the tracking gain, k_p, for stability. This limit is derived in Eqn. (9)

$$H_{den}(s) = s^3 + (2\zeta\omega_n - dk)s^2 + (\omega_n^2 - 2\zeta\omega_n dk)s + k(k_p\sigma^2 - d\omega_n^2 - \sigma^2). \quad (2)$$

where $_{num}/_{den}$ denote the numerator and denominator of the transfer function.

3.1 Choice of feed-through

The feed-through term, d, is chosen to make the system type 1. The type number of a system is defined as the number of poles at the origin in the systems loop gain transfer function. A type 1 system will provide a steady state error of zero when tracking step inputs. As IRC provides a type 1 system, the modified IRC scheme must also be made type 1 to prevent performance degradation.

Consider the type 0 system given in Eqn. (2). The system becomes type 1 if the coefficients of both the numerator and denominator s^0 terms are equal, i.e.

$$\begin{aligned} k(k_p\sigma^2 - d\omega_p^2 - \sigma^2) &= k_p k\sigma^2 \\ \Rightarrow -d\omega_n^2 - \sigma^2 &= 0. \end{aligned} \quad (3)$$

As ω_n and σ are plant parameters and cannot be changed, Eqn. (3) is only satisfied if d is chosen to be $d = -\sigma^2/\omega_n^2$, which will be denoted as d_n. In order to introduce a zero at the origin, σ and ω_n must be measured accurately. If d is not sufficiently accurate, the zero will move from the origin.

Choosing $d = d_n$, the plant plus feed-through is as follows

$$G(s) + d_n = \frac{ds(s + 2\zeta\omega_n)}{s^2 + 2\zeta\omega_n s + \omega_n^2} \quad (4)$$

which has zeros at $s = 0, -2\zeta\omega_n$. When the damping controller is implemented, the pole introduced at $s = 0$ cannot move beyond the zero at the origin for any damping gain, k. The modified IRC relies on the zero at the origin, to ensure correct pole placement.

Substituting Eqn. (3) into the transfer function of the IRC damping loop gives

$$G_{IRC}(s) = \frac{k\sigma^2}{s(s^2 + (2\zeta\omega_n - dk)s + (\omega_n^2 - 2\zeta\omega_n dk))}. \quad (5)$$

The system has a real pole at $s = 0$, as well as two additional poles. The additional poles will be complex if the following is true

$$\begin{aligned} &(2\zeta\omega_n - dk)^2 - 4(\omega_n^2 - 2\zeta\omega_n dk) < 0 \\ &\Rightarrow d^2k^2 + 4\zeta\omega_n dk + 4(\zeta^2 - 1)\omega_n^2 < 0. \end{aligned} \quad (6)$$

Neglecting ζ terms for simplicity gives

$$k < \frac{2\omega_n^3}{\sigma^2}. \quad (7)$$

Choosing k such that the IRC loop has only one real pole ensures the real pole will be $s = 0$. The loop gain of the damped and tracked system is then

$$\frac{k_p k\sigma^2}{s(s^2 + (2\zeta\omega_n - dk)s + (\omega_n^2 - 2\zeta\omega_n dk))} \quad (8)$$

and so, the system becomes type 1.

Using the Routh-Hurwitz stability criterion, it is found that to ensure stability, the following limitations must be placed on k_p

$$0 < k_p < \frac{(\omega_n^2 - 2\zeta\omega_n dk)(2\zeta\omega_n - dk)}{k\sigma^2}. \quad (9)$$

4. OPTIMISATION FOR FLAT BAND RESPONSE

In nanopositioning, the most commonly used input signal is a triangle wave. The triangle wave consists of infinite harmonics of the base frequency. A system with flat band response is desirable as it most accurately recreates the harmonics of the reference signal within its bandwidth. In this section, the controller gains which provide a flat band response are found. This is done by finding the turning points of the FRF, deriving the conditions for which the difference in magnitude at the turning points is minimal, and finally, calculating the controller parameters such that the input-harmonic-weighted frequency response

$$\left| \sum_{i=1,3,5,\ldots}^{\infty} \frac{-1^{\frac{i-1}{2}}}{i^2} \left|H(j\omega_i)\right|_{dB} \right| \quad (10)$$

is minimised, where ω_i is the i-th harmonic of the input signal, and $|\cdot|_{dB} = 20\log_{10}|\cdot|$. This is equivalent to a magnitude of 0 dB at the turning points, which will be used in the analysis.

4.1 Turning Points of the FRF

The FRF $|H(j\omega)|$ has five turning points. One occurs at $\omega = 0$, which will be discounted from analysis as the type number of the system guarantees a magnitude of 0 dB at this point. Additionally, it is known that $G(-j\omega) = G(jw)^*$, therefore, $|G(-j\omega)| = |G(j\omega)|$. Thus, of the four remaining turning points, there are two pairs with equal magnitude and opposite sign. For this reason, only the two positive roots will be considered. Neglecting ζ terms, for simplicity, in the transfer function of the modified IRC scheme gives the simplified system, H_s,

$$H_s(j\omega) = \frac{k_p k\sigma^2}{(dk\omega^2 + k_p k\sigma^2) + j(\omega_n^2\omega - \omega^3)}. \quad (11)$$

The turning points occur when

$$\frac{\delta}{\delta\omega}\left|H_s(j\omega)\right| = 0. \quad (12)$$

Solving this equation gives the frequency at which the turning points occur as

$$\omega_{tp} = \sqrt{\frac{2\omega_n^2 - d^2k^2 \pm \sqrt{d^4k^4 - 4d^2k^2\omega_n^2 - 6dk_pk^2\sigma^2 + \omega_n^4}}{3}}. \quad (13)$$

4.2 Minimising the Difference in Magnitude at ω_{tp}

Making the substitution

$$\Delta = \sqrt{d^4k^4 - 4d^2k^2\omega_n^2 - 6dk_pk^2\sigma^2 + \omega_n^4}, \quad (14)$$

into Eqn. (13) gives

$$\omega_{tp} = \sqrt{\frac{2\omega_n^2 - d^2k^2 \pm \Delta}{3}}. \quad (15)$$

It is clear that for $\Delta = 0$, will have two equal solutions, and so there will be no difference in the magnitude. However, in order to find any other conditions which minimise the difference in magnitude, the following must be solved

$$|H_s(j\omega_{tp_{max}})| - |H_s(j\omega_{tp_{min}})| = 0. \quad (16)$$

This is found to be true only for

$$|\Delta| = 0$$

Using Eqn. (14), this can be solved for the tracking gain, k_p, giving

$$k_p = \frac{d^4k^4 - 4d^2k^2\omega_n^2 + \omega_n^4}{6dk^2\sigma^2}.$$

4.3 Calculating Controller Parameters

For the condition $\Delta = 0$, the solutions of Eqn. (13) are real and equal. Therefore the FRF of any modified IRC scheme such that Eqn. (17) is true, does not have turning points but a point of inflection. This does not guarantee a flat band response. In order for this to happen, the magnitude at the point of inflection must be sufficiently close to 0 dB. Substituting $\Delta = 0$ into Eqn. (15) gives

$$\omega_{tp} = \sqrt{\frac{2\omega_n^2 - d^2k^2}{3}}. \quad (17)$$

The optimal damping gain, k, is found by solving $|H_s(j\omega_{tp})| = 1$.

$$|H_s(j\omega_{tp})| = \frac{k_p k\sigma^2}{\sqrt{\frac{-9d^6k^6 + 54d^4\omega_n^2k^4 - 108d^2\omega_n^4k^2 + 72\omega_n^6 + 81k_p^2k^2\sigma^4}{81}}} \quad (18)$$

which is equal to 1 when

$$\begin{aligned} &\frac{-9d^6k^6 + 54d^4\omega_n^2k^4 - 108d^2\omega_n^4k^2 + 72\omega_n^6}{81} \\ &= k^6 - 6d^{-2}\omega_n^2k^4 + 12d^{-4}\omega_n^4k^2 - 8d^{-6}\omega_n^6 \\ &= (k^2 - 2d^{-2}\omega_n^2)^3 = 0. \end{aligned} \quad (19)$$

This gives the following controller parameters

$$k = \sqrt{2}\frac{\omega_n^3}{\sigma^2},\ k_p = 0.25.$$

4.4 Adaptation for Implementation

The control scheme developed in the previous sections, though plausible in theory, is limited in terms of performance in application. This is due to the use of a proportional tracking controller. A tracking controller with integral action provides many benefits in practice. The system is more robust against perturbations in the plant and disturbances. Integral tracking action has also been shown to reduce the effect of nonlinear behaviours, such as hysteresis and creep, to an acceptable level [Bhikkaji et al. (2007); Devasia et al. (2007); Aphale et al. (2008); Fleming (2010)].

To add integral action to the tracking controller, first the feedtrough term is reduced to slightly less than d_n. This causes the damping controller induced pole to move into the left half plane, without significantly changing the position of the damped poles. A structured PI controller is used, see Teo et al. (2014), of the form

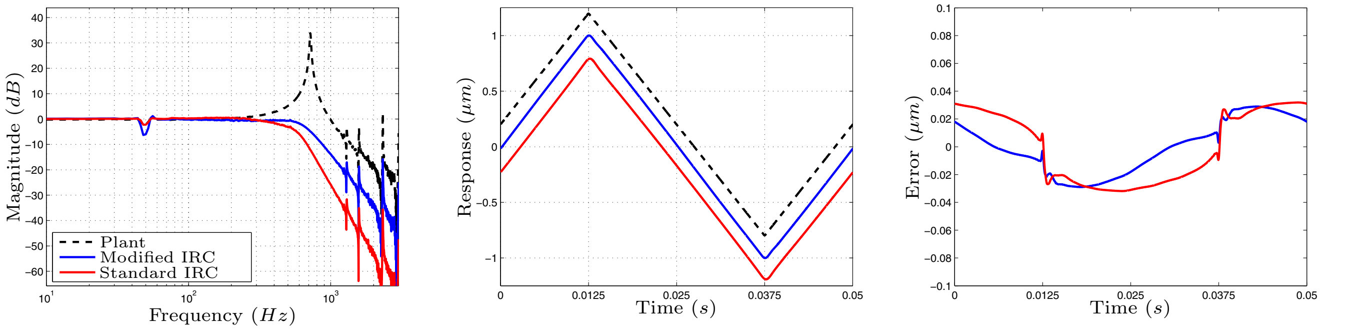

(a) (b) (c)

Fig. 3. (a) Bode magnitude plot for the plant, standard, and modified IRC schemes. (b) Simulated response of each of the IRC schemes to an input of a 20 Hz triangle wave of amplitude ± 1 μm, offset by 0.2 μm for clarity, and time-shifted to compensate for phase differences. (c) Error signals for both the standard and modified IRC schemes.

$$C_t(s) = \frac{k_p(s+p)}{s} \tag{20}$$

where p is the location of damping controller induced pole and is given by

$$\begin{aligned} p &= -(A + B - \frac{a}{3}),\ \ a = 2\zeta\omega_n - dk, \\ b &= \omega_n^2 - 2\zeta\omega_n dk,\ \ c = -k(d\omega_n^2 + \sigma^2), \\ Q &= \frac{a^2 - 3b}{9},\ \ R = \frac{2a^3 - 9ab + 27c}{54}, \\ A &= -\sqrt[3]{R + \sqrt{R^2 - Q^3}},\ \ B = \frac{Q}{A}. \end{aligned} \tag{21}$$

5. SIMULATION

Simulations are carried out using the measured frequency response of a two-axis serial kinematic nanopositioner designed and constructed at the EasyLab, University of Nevada, Reno. The stage is driven by a Piezodrive PDL200 200 V linear amplifier, and the position measured using a Microsense 4810 capacitive sensor. The frequency response is measured using an Agilent 35670A Dynamic Signal Analyzer.

The second-order model is derived from the measured frequency response using the discrete time system identification algorithm described in McKelvey et al. (1996). The continuous time model is then found by bilinear transform giving

$$G(s) = \frac{2.036 \times 10^7}{s^2 + 80.67s + 2.036 \times 10^7}. \tag{22}$$

The standard IRC damping controller is designed using the method laid out in Namavar et al. (2013), and the modified IRC damping controller using the method laid out in this paper. In simulation, using the measured frequency response data, both schemes suffered significantly reduced bandwidth due to the resonant modes not accounted for in the second order model. The tracking controller gains were adjusted, via trial and error, to obtain maximum bandwidth in each case. The final controller designs are listed in the following table.

	Standard	Modified
d	-2	-1.05
C_d	$\frac{2683}{s}$	$\frac{6381}{s}$
C_t	$\frac{1200}{s}$	$\frac{0.37s+128.8}{s}$

Fig. 3 shows the simulated results of both the standard and modified IRC designs. The resulting bandwidth and error measurements are presented in the following table.

	Standard	Modified
Bandwidth ± 1 dB (Hz)	346	546
Bandwidth ± 3 dB (Hz)	482	654
Max. Error (V)	0.0319	0.0290
RMS Error (V)	0.0252	0.0188

5.1 Robustness

To verify performance in the presence of plant perturbations, simulations were carried out using the measured frequency response of the platform with a 10 g mass added. The addition of the mass causes the first resonant frequency to reduce from 718 Hz to 596 Hz. The simulated response is shown in Fig. 4 and the results are as follows:

	Standard	Modified
Bandwidth ± 1 dB (Hz)	448	450
Bandwidth ± 3 dB (Hz)	452	546
Max. Error (V)	0.0455	0.0756
RMS Error (V)	0.0285	0.0374

.

6. CONCLUSION

In this paper, a modified IRC scheme is introduced with the aim to increase the positioning bandwidth of lightly damped resonant systems. A method for reducing the order of the controller through a selective choice of feedthrough is found. This is incompatible with standard IRC. Controller parameters have been analytically derived in order to provide maximum tracking bandwidth. Simulations show substantial improvements in tracking bandwidth over standard IRC designs, though the improvement is reduced for large perturbations of the plant.

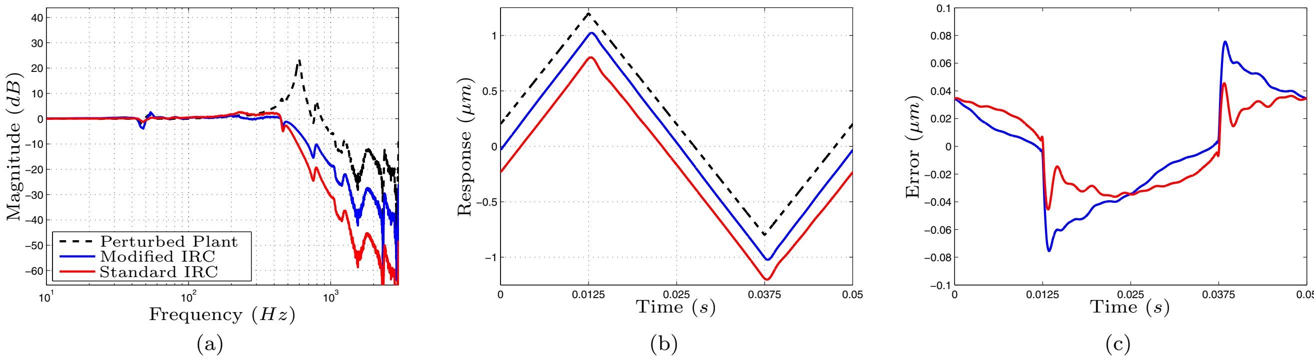

Fig. 4. (a) Bode magnitude plot for the perturbed plant, standard, and modified IRC schemes. (b) Simulated response of each of the IRC schemes to an input of a 20 Hz triangle wave of amplitude ± 1 μm, offset by 0.2 μm for clarity, and time-shifted to compensate for phase differences. (c) Error signals for both the standard and modified IRC schemes.

REFERENCES

S. S. Aphale, A. J. Fleming, and S. O. R. Moheimani. Integral resonant control of collocated smart structures. *Smart Materials and Structures*, 16:439 – 446, February 2007.

S. S. Aphale, B. Bhikkaji, and S. O. R. Moheimani. Minimizing scanning errors in piezoelectric stack-actuated nanopositioning platforms. *IEEE Transactions on Nanotechnology*, 7(1):79–90, 2008.

B. Basu and S. R. K. Nielsen. A multi-modal control using a hybrid pole-placementintegral resonant controller (ppir) with experimental investigations. *Structural Control and Health Monitoring*, 18:191 – 206, 2011.

B. Bhikkaji, M. Ratnam, A. J. Fleming, and S. O. Reza Moheimani. High-performance control of piezoelectric tube scanners. *IEEE Transactions on Control Systems Technology*, 15(5):853 – 866, September 2007.

S. Devasia, E. Eleftheriou, and S. O. R. Moheimani. A survey of control issues in nanopositioning. *IEEE Transactions on Control Systems Technology*, 15(4):689 – 703, July 2007.

I. M. Diaz, E. Pereira, and P. Reynolds. Integral resonant control scheme for cancelling human-induced vibrations in light-weight pedestrian structures. *Structural Control and Health Monitoring.*, 19(1):55–69, 2012.

J. L. Fanson and T. K. Caughey. Positive position feedback control for large space structures. *AIAA Journal*, 28(4): 717 – 724, 1990.

A. J. Fleming. Nanopositioning system with force feedback for high-performance tracking and vibration control. *IEEE / ASME Transactions on Mechatronics*, 15(3): 433–447, 2010.

A. J. Fleming, S. S. Aphale, and S. O. R. Moheimani. A new method for robust damping and tracking control of scanning probe microscope positioning stages. *IEEE Transactions on Nanotechnology*, 9(4):438 – 448, 2010.

P. P. Friedmann and T. A. Millott. Vibration reduction in rotorcraft using active control: A comparison of various approaches. *Journal of Guidance, Control and Dynamics*, 18(4):664 – 673, 1995.

S. C. P. Gomes, V. S. da Rosa, and B. de Carvalho Albertini. Active control to flexible manipulators. *IEEE/ASME Transactions on Mechatronics*, 11(1):75–83, 2006.

D. J. Inman. *Vibration with Control, Measurement, and Stability*. Englewood Cliffs, NJ: Prentice-Hall, 1989.

T. McKelvey, H. Akcay, and L. Ljung. Subspace based multivariable system identification from frequency response data. *IEEE Tansaction on Automatic Control*, 41(7):960–979, 1996.

M. Namavar, A. J. Fleming, M. Aleyaasin, K. Nakkeeran, and S. S. Aphale. An analytical approach to integral resonant control of second-order systems. *in press, IEEE Transactions on Mechatronics*, 2013.

H. Numasato and M. Tomizuka. Settling control and performance of a dual-actuator system for hard disk drives. *IEEE/ASME Transactions on Mechatronics*, 8 (4):431–438, 2003.

E. Pereira, S. S. Aphale, V. Feliu, and S. O. R. Moheimani. Integral resonant control for vibration damping and precise tip-positioning of a single-link flexible manipulator. *IEEE / ASME Transactions on Mechatronics*, 16(2):232 – 240, April 2011.

H. R. Pota, S. O. R. Moheimani, and M. Smith. Resonant controllers for smart structures. *Smart Materials and Structures*, 11:1 – 8, 2002.

A. Preumont. *Vibration Control of Active Structures: An Introduction*. Dordrecht: Kluwer, 1997.

S. Salapaka, A. Sebastian, J. P. Clevland, and M. V. Salapaka. High bandwidth nano-positioner: A robust control approach. *Review of Scientific Instruments*, 73 (9):3232 – 3241, September 2002.

A. Sebastian, A. Pantazi, S. O. R. Moheimani, H. Pozidis, and E. Eleftheriou. Achieving sub-nanometer precision in a mems storage device during self-servo write process. *IEEE Transactions on Nanotechnology*, 7(5):586 – 595, September 2008.

Y. R. Teo, D. Russell, S. S. Aphale, and A. J. Fleming. Improved integral force feedback and structured pi tracking control: Application for high speed confocal microscopy. *Submitted to Proc. of the IFAC World Congress 2014, Invited Session on Dynamics and Control of Micro and Nano Systems I*, 2014.

S. P. Wadikhaye, B. Bhikkaji, S. O. R. Moheimani, and Y. K. Yong. Analog implementation of a damping and tracking controller for a high-speed x-y nanopositioner. In *American Control Conference*, pages 3811 – 3816, 2012.